In situ electrochemical analysis of anthocyanin activation by ROS in blueberries

Antonio Doménech-Carbó*[a], Irene Domínguez[b]

[a] Departament of Analytical chemistry, University of Valencia, Dr. Moliner 50, 46100 Burjassot, València, Spain.

[b] Department of Agroindustry and Food Quality, Andalusian Institute of Agricultural and Fisheries Research and Training (IFAPA), La Mojonera, Camino San Nicolás, 1, Almeria, E-04745, Spain. e-mail: irene.dominguez.perez@juntadeandalucia.es

* Corresponding author; e-mail: antonio.domenech@uv.es.
ORCID: 0000-0002-5284-2811.
(Phone: +34-963544533; Fax: +34-963544436)

Abstract

The in situ voltammetry of blueberry fruits and microparticulate deposits from their ethanolic extracts reveals the appearance of a prominent oxidation signal at ca. –0.7 V vs. Ag/AgCl which only appears in the presence of O_2 in conditions in which superoxide radical anion is generated initially. These features, mainly associated to anthocyanins, are in agreement with SECM examination of blueberry thin epithelial films, and suggest that there is a ROS-assisted promotion of the antioxidant capacity of anthocyanins accompanying the phenoxide-mediated ROS reactivity of these compounds.

Keywords: Blueberry; Anthocyanins; Electrochemistry; ROS activation.

1. Introduction

Anthocyanins are plant polyphenolic pigments widely distributed in fruits and flowers, responsible for their red, blue and purple hues. These compounds, which can be ascribed to the flavonoid family, exhibit reactive oxygen species (ROS) scavenging activity and play an important role in protecting higher plants against photochemical and biochemical damage [1].

Anthocyanins, and flavonoids in general, are believed to donate hydrogen atoms from phenoxyl groups to radicals, thus inactivating their oxidate activity via hydrogen atom transfer, sequential proton loss electron transfer, and single electron transfer followed by proton transfer mechanisms [2]. Anthocyanin accumulation in plants can be triggered by many chemical and environmental factors, including ROS. However, the mechanism of ROS-induced anthocyanin accumulation and the role of anthocyanins in signaling pathways that determine plant response to different stresses are largely unknown [3].

Despite the difficulty due to the enormous variety of plant components participating in plant metabolic cycles, electrochemical techniques play an important role in plant physiology studies [4]. These include *in situ* voltammetry approaches, mainly concentrated in monitoring H_2O_2 and other signaling species [5].

In this context, we studied the application of voltammetry to monitor polyphenolic components in plants to obtain physiological [6], chemoecological [7], and phylogenetic [8] information via *in situ* voltammetry [9] and adapting solid state electrochemistry methods (voltammetry of immobilized particles, VIMP) to plant extracts [6-8]. The rich aqueous electrochemistry of much flavonoids is dominated by the 2-proton, 2-electron oxidation of *o*-catechol groups to the corresponding *o*-quinones, often be accompanied by the oxidation of the 5,7-dihydroxyl groups, at higher potentials and oxidation with opening of the ring C [10-13]. At physiological pHs, the corresponding voltammetric features are concentrated in the region of potentials between 0.0 and 1.2 V vs. Ag/AgCl. The interaction of flavonoids with ROS, however, has been concentrated in studies in organic solvents where superoxide radical anion is reversibly formed [14-16].

Here, we present a study of the anthocyanidin-related electrochemistry of blueberry fruits based on in situ analysis via insertion of microelectrodes into the fruits, voltammetric analysis of fruit extracts and scanning electron microscopy (SECM) study of anthocyanidin-rich epithelial films. The extension of the potential range to values where superoxide ion and other ROS are subsequently generated [17,18] expands the available analytical information [6,9,19]. Comparing electrochemical data in O_2-rich and O_2-free conditions leads as a result, in contrast with the electrochemistry in aprotic media [14-16], the generation of species with considerably lower oxidation potential. This means that the interaction with ROS activates the antioxidant capabilities of anthocyanins.

2. Experimental

Blueberry fruits were purchased from commercial suppliers in Burjassot (Valencia). *In situ* voltammetry was performed by inserting platinum (diameter 25 μm) and graphite (0.5 mm diameter) electrodes. These were alternatively used as working electrodes completing the three-electrode arrangement with platinum auxiliary and pseudoreference microelectrodes (100 μm diameter). All electrodes were inserted perpendicularly into the blueberry fruit to a depth of 2 mm forming a triangle with 2 mm spacings between them. The potential of the Pt pseudoreference microelectrodewas calibrated vs. Ag/AgCl (3 M NaCl) by means of cyclic vooltammograms at platinum and graphite microelectrodes in 1.0 mM $K_3Fe(CN)_6$ plus 1.0 mM $K_4Fe(CN)_6$ solution in aqueous 0.10 M KCl.

Voltammetry of microparticulate deposits resulting from the evaporation of ethanolic extracts on glassy carbon electrode (GCE) were prepared from macerated blueberry fruits as already described [6-8]. 0.10 M aqueous potassium phosphate buffer at pH 7.4 was used as electrolyte solution optionally deaerated by bubbling Ar, eventually adding DMSO. All these measurements, as well as SECM ones were carried out with a CH 920c potentiostat in three-electrode configuration with Ag/AgCl (3 M NaCl) reference electrode and Pt-wire counter electrode. SECM imaging was obtained on thin film (surface area ca. 2 mm^2) of the ephitelial region of fruits extracted with a scalpel and deposited over a graphite paste (50% wt graphite plus 50% wt nujol oil) bed covering a Pt substrate electrode (geometrical area 0.018 cm^2). A Pt microelectrode tip (CH 49,

diameter 20 μm) was used. The rate of scanning of the tip over the substrate was 20 μm s^{-1} for all experiments, the distance between tip and substrate being of the order of the tip electrode radius. 2.5 mM $K_3Fe(CN)_6$ plus 2.5 mM $K_4Fe(CN)_6$ solution in air-saturated phosphate buffer at pH 7.4 was used as the electrolyte solution.

3. Results and discussion

Figure 1 shows the square wave voltammograms (SWVs) of microparticulate deposits of ethanolic extracts from blueberry fruits on GCE in contact with air-saturated and deoxygenated phosphate buffer aqueous solutions at pH 7.4. Both voltammograms exhibit a series of overlapping anodic peaks (A) between –0.2 and 1.0 V vs. Ag/AgCl which can be attributed to the oxidation of polyphenolic compounds, being the most abundant anthocyanins pelargonidin-3-*O*-glucoside, peonidin-3-*O*-rutinoside and delphinidin-3-*O*-rutinoside [1,20]. These processes can be ascribed to the aforementioned oxidation of *o*-catechol units and processes involving the opening of the C-ring [10-13]. These are as illustrated for delphinidin in Scheme 1.

Remarkably, in the voltammograms at blueberry-modified GCE in O_2-containing solutions, a prominent additional peak appears at –0.7 V (A*), as can be seen in Figure 1. Notice that the voltammograms in this figure are taken on different microparticulate deposits from blueberry extracts using the VIMP methodology [7,8]. Since there is no possibility of controlling the net amount of sample attached to the base electrode, the relative intensity of the A and A* signals rather than their absolute values have to be compared. The peak A* disappears upon deoxygenation of the electrolyte solution denoting that oxygen species are involved in its generation. However, the signal A* does not appear at unmodified GCE in O_2- and H_2O_2-containing solutions, thus denoting that cannot be attributed to an oxygen species electrochemically generated. Similar features were recorded in blank experiments in pelargonidin, cyaniding and delphinidin solutions in phosphate buffer (Figure 2a,b). Here, the voltammetry again consists exclusively of oxidation A-peaks in deoxygenated solutions whereas the A* signal is reproduced in the presence of dissolved oxygen and decreases upon deoxygenation (see Figure 2c). This suggests that local pH changes associated to the deposited particles cannot be responsible for the observed voltammetry.

These results exhibit several significant differences with studies on the interaction of ROW with phenolic compounds in aprotic solvents [14-16]. Here, the well-known one-electron reversible reduction of O_2 to superoxide ($O_2 + e^- \rightarrow O_2^{\bullet -}$) is followed by the reaction of this species with the polyphenolic component. This results in the enhancement or decrease of the voltammetric signals for the O_2/ $O_2^{\bullet -}$ couple and the HA-localized signals. In the case of flavonoids such as quercetin and anthocyanins, these processes involve the hydrogen atoms of the *o*-catechol groups. This 'ordinary' pathway is represented in Scheme 1 by the red line path.

The features observed in aqueous media can be interpreted taking into account that, under our experimental conditions dissolved oxygen is reduced ca. –0.70 V, the initial step is the one-electron reduction of O_2 to superoxide radical anion ($O_2 \cdot^-$), which subsequently experiences protonation to give hydroperoxide radical ($HO_2 \cdot$) competing with other processes yielding hydroxyl radical ($HO \cdot$), hydrogen peroxide and, ultimately, water through a cascade mechanism [21,22]. Accordingly, the peak A* can be attributed to the oxidation of a species generated by reaction of the parent anthocyanin with electrochemically generated superoxide radical anion but also other ROS. Consistently with this picture, the height of the signal A* recorded in microparticulate deposits of ethanolic extracts from blueberry fruits (Figure 2c,d) as well as on delphinidin, cyanidin and palrgonidin solutions in phosphate buffer increases on initiating the potential scan at more negative potentials and decreases upon adding DMSO (see Figure 2d), a recognized radical scavenger [23].

In situ SWV at Pt microelectrodes inserted into blueberry fruits is illustrated in Figure 3. Here, the signal A* is particularly intense and is accompanied by other intense signals at ca. –0.40 and –0.50 V whose intensity increases with increasing frequency. These features can be interpreted by considering that the insertion of the electrodes facilitates the aeration of the system and initiates the defense response of the fruit. Accordingly, different ROS are chemically (signaling pathways) and electrochemically generated and they can react with anthocyanidin species in the vicinity of the electrode surface. The variation of the voltammetric profile with the frequency can be interpreted as resulting from the formation of different ROS from the initially generated superoxide, according

to the aforementioned a cascade mechanism [21,22]. It is conceivable that the relative proportions –and hence, the respective reaction products with anthocyanins– of superoxide, hydroperoxide, hydroxyl, etc. species will vary with the characteristic time of the experiment.

SECM experiments using the redox competition strategy [24] were consistent with the above considerations. Figure 4 shows the color plots and topographic SECM images of a thin epithelial film using $Fe(CN)_6^{3-}/Fe(CN)_6^{4-}$ redox probe in air-saturated phosphate buffer at pH 7.4. The potential applied to the tip (E_T) was of 0.30 V, corresponding to the diffusion-controlled oxidation of $Fe(CN)_6^{4-}$ to $Fe(CN)_6^{3-}$. When no potential was applied to the blueberry substrate (a,c) the tip reflects more or less intense negative feedback features associated to the more or less thickness of the film. When (b,d) a potential negative enough to produce the reduction of dissolved oxygen in the regions where the bare graphite paste is exposed to the air-saturated electrolyte, is applied to the substrate (E_S = −1.0 V), there are significant changes in the SECM response. The gross (green) region of the film becomes apparently narrowed and the tip current increases in the boundary of the same with the thin (brown) region which, in turn, is apparently smoothed. These features can be interpreted by assuming that the ROS electrochemically generated react with the anthocyanin components of the film exposed to the electrolyte in the thin region and in the presumably fractured region between the thin and thick regions of the film. The generation of new species, some of which pass to the solution will determine conductivity changes shifting the tip current.

Scheme 1 depicts a tentative multiple reaction pathway aimed to interpret the above voltammetric and SECM data taking delphinidin as representative anthocyanin. For simplicity, the superoxide radical anion was taken as the reacting ROS. In principle, the reaction of anthocyanins with superoxide ion can proceed similarly as described in aprotic media (red line in Scheme 1) yielding either a radical or an anion [14-16] whose electrochemical oxidation occurs via *o*-catechol to *o*-quinone transformation. This last corresponds to the A-processes recorded in aqueous electrolytes (Figures 1-3) being equivalent to the redox processes in aprotic media.

A second candidate to be responsible for process A* can be any peroxo-bridged species formed by reaction with superoxide (and/or other superoxide-type ROS). Their formation by direct reaction with peroxo species [25] and electroactive character [19] was described for quercetin. The corresponding reaction pathway is summarized in the blue line of Scheme 1. Again, however, the electrochemical oxidation involves the *o*-catechol to *o*-quinone transformation presumably occurring at relatively high potentials; i.e., as A-signals. A third reaction pathway (green line in Scheme 1) can involve anthocyanin ring opening, but it is conceivable that this process was not favored in terms of oxidation potentials. None of the above species resulting from the oxidation of anthocyanins appear to provide the high degree of electronic conjugation demanded for the signal A*. Tentatively, one can hypothesize that the more extensive reorganization embedded into the grey zone in Scheme 1 provides finally an oxidized form with high electronic conjugation compatible with the low oxidation potential of its precursor. Obviously, however, this is highly speculative at the current stage of the study.

Conjointly considered, these results depict a new scenario for the recognized radical scavenging activity of anthocyanins where the reaction with ROS yields species with high antioxidant capacity.

4. Final considerations

In situ voltammetry of blueberry fruits, combined with voltammetry of ethanolic extracts and redox-competitive SECM, reveal sharp differences between the electrochemistry in the presence and absence of O_2. These data are consistent with the activation of the antioxidant capacity of anthocyanins by ROS and the appearance of alternative pathways in the radical scavenging activity of these compounds.

Acknowledgments: Financial support by the project PID2020-113022GB-I00 within the MCIN/ AEI /10.13039/50110 0 011033 frame is gratefully acknowledged.

References

[1] L. Fan, L. Lin, Y. Zhang, S. Li, Z. Tang, Component characteristics and reactive oxygen species scavenging activity of anthocyanins from fruits of *Lonicera caerulea* ,. Food Chem. 403 (2023) 134391.

[2] G. Litwinienko, K.U. Ingold, Solvent effects on the rates and mechanisms of reaction of phenols with free radicals, Acc. Chem. Res. 40 (2007) 222–230.

[3] Z. Xu, K. Mahmood, S.J. Rothstein, ROS Induces Anthocyanin Production Via Late Biosynthetic Genes and Anthocyanin Deficiency Confers the Hypersensitivity to ROS-Generating Stresses in Arabidopsis, Plant Cell Physiol. 58 (2017) 1364-1377.

[4] A.G. Volkov, Ed., Plant Electrophysiology. Signaling and Responses, Springer, Berlin, 2012.

[5] Q.-Q. Ren, X.-R. Huang, G.-C. Liu, O.-Y. Jun, M.-T. Li, H. Chen, Y.-D. Zhao, W. Chen, A field-compatible technique using an electrochemical sensing microbundle for real-time and simultaneous in vivo measurement of hydrogen peroxide, nitric oxide, and pH under drought stress, Sens. Actuator B 220 (2015) 743–748.

[6] A. Doménech-Carbó, N. Montoya, P. Soriano, E. Estrelles, An electrochemical analysis suggests role of gynodioecy in adaptation to stress in *Cortaderia selloana*, Curr. Plant Biol. 16 (2018) 9–14.

[7] A. Doménech-Carbó, G. Cebrián_Torrejón, A. Lopes-Souto, M. Martins de Moraes, M. Jorge-Kato, J. Fechine-Tavares, J.M. Barbosa-Filho, Electrochemical ecology: VIMP monitoring of plant defense against external stressors, RSC Adv. 5 (2015) 61006–61011.

[8] A. Doménech-Carbó, A.M. Ibars, J. Prieto-Mossi, E. Estrelles, F. Scholz, G. Cebrián-Torrejón, M. Martini, Electrochemistry-based chemotaxonomy in plants using the voltammetry of microparticles methodology, New J. Chem. 39 (2015) 7421–7428.

[9] A. Doménech-Carbó, D. Dias, M. Donnici, In vivo electrochemical monitoring of signaling transduction of plant defense against stress in leaves of *Aloe vera* L., Electroanalysis 33 (2021) 1024–1032.

[10] A.K. Timbola, C.D. de Souza, C. Giacomelli, A. Spinelli, Electrochemical oxidation of quercetin in hydro-alcoholic solution, J. Braz. Chem. Soc. 17 (2006) 139–148.

[11] P. Janeiro, A.M. Oliveira-Brett, Redox Behavior of Anthocyanins Present in *Vitis vinifera* L. Electroanalysis 19 (2007) 1779–1786.

[12] A. Masek, E. Chrzescijanska, M. Zaborski, Electrooxidation of morin hydrate at a Pt electrode studied by cyclic voltammetry, Food Chem. 148 (2014) 18–23.

[13] A.-M. Chiorcea-Paquim, T.A. Enache, E. De Souza Gil, A.M. Oliveira-Brett, Natural phenolic antioxidants electrochemistry: Towards a new food science methodology. Comprehensive Reviews in Food Chemistry and Food Safety 19 (2020) 1680–1726.

[14] A. René, M.-L. Abasq, D. Hauchard, P. Hapiot, How Do Phenolic Compounds React toward Superoxide Ion? A Simple Electrochemical Method for Evaluating Antioxidant Capacity, Anal. Chem. 82 (2010) 8703–8710.

[15] S.J.L. Lauw, Z. Chiang, J.H.Q. Lee, R.D. Webster, Comparing the Relative Reactivities of Structurally Varied Alcohols toward Electrochemically Generated Superoxide, ChemElectroChem 5 (2018) 643–650.

[16] D. Jadreško, A. Miličević, I. Novak Jovanović, Reactivity of flavonoids toward superoxide radical: An electrochemical approach, Electrochim. Acta 421 (2022) 140501.

[17] T.A. Enache, A.M. Chiorcea-Paquim, O. Fatibello-Filho, A.M. Oliveira-Brett, Hydroxyl radicals electrochemically generated in situ on a boron doped diamond electrode, Electrochem. Commun. 11 (2009) 1342–1345.

[18] A. Kapałka, G. Foti, C. Comninellis, The importance of electrode material in environmental electrochemistry: Formation and reactivity of free hydroxyl radicals on boron-doped diamond electrodes, Electrochim. Acta 54 (2009) 2018–2023.

[19] A. Doménech-Carbó, R. Gavara, P. Hernández-Muñoz, I. Domínguez, Contact probe voltammetry for in situ monitoring of the reactivity of phenolic tomato (solanum lycopersicum L.) compounds with ROS, Talanta 144 (2015) 1207–1215.

[20] A.M. Mustafa, S. Angeloni, D. Abouelenein, L. Acquaticci, J. Xiao, G. Sagratini, F. Maggi, S. Vittori, G. Caprioli, A new HPLC-MS/MS method for the simultaneous determination of 36 polyphenols in blueberry, strawberry and their commercial products and determination of antioxidant activity, Food Chem. 367 (2022) 130743.

[21] J. Xu, W. Huang, R.L. McCreery, Isotope and surface preparation effects on alkaline dioxygen reduction at carbon electrodes, J. Electroanal. Chem. 410 (1996) 235–242.

[22] I. Katsounaros, W.B. Schneider, J.C. Meier, U. Benedikt, P.U. Biedermann, A.A. Auer, K.J. Mayrhofer, Hydrogen peroxide electrochemistry on platinum: towards understanding the oxygen reduction reaction mechanism, PhysChemChemPhys 14 (2012) 7384-7391.

[23] R. Herscu-Kluska, A. Masanwa, M. Saphier, H. Cohen, D. Meverstein, Mechanism of the reaction of radicals with peroxides and dimethyl sulfoxide in aqueous solution, Chem. 14 (2008) 5880–5890.

[24] K. Karnicka, K. Eckhard, D.A. Guschin, L. Stoica, P. J. Kulesza, W. Schumann, Visualisation of the local bio-electrocatalytic activity in biofuel cell cathodes by means of redox competition scanning electrochemical microscopy (RC-SECM), Electrochem. Commun. 9 (2007) 1998-2002.

[25] V. Krishnamachari, L.H. Levine, P.W. Paré, Flavonoid oxidation by the radical ge5erator AIBN: a unified mechanism for quercetin radical scavenging, J. Agric. Food Chem. 50 (2002) 4357–4363.

Figures

Figure 1. SWVs of two different microparticulate deposits of ethanolic extracts from blueberry fruits on GCE in contact with air-saturated (black) and deoxygenated (red) 0.10 M phosphate buffer at pH 7.4. Potential scan initiated at −1.05 V in the positive direction; potential step increment 4 mV; square wave amplitude 25 mV; frequency 5 Hz. The arrow marks the direction of the potential scan.

Figure 2. SWVs of: a) 0.5 mM pelargonidin plus 0.5 mM delphinidin, and b) 0.5 mM pelagonidin plus 0.5 mM cyanidin in air-saturated phosphate buffer. SWVs of different microparticulate deposits of ethanolic extracts from blueberry fruits in contact with phosphate buffer c) in different steps during the progressive deoxygentation of the electrolyte solution; and d) phosphate buffer solution (black line) and phosphate buffer plus DMSO (10% v/v) solution (red line). Potential scan initiated at −1.05 V in the positive direction; potential step increment 4 mV; square wave amplitude 25 mV; frequency 5 Hz. The arrow marks the direction of the potential scan.

Figure 3. *In situ* SWVs at Pt microelectrode of blueberry fruits at different frequencies. Potential scan initiated at −0.85 V in the positive direction; potential step increment 4 mV; square wave amplitude 25 mV. The arrow marks the direction of the potential scan.

Figure 4. Color plots (a,b) and topographic SECM images (c,d) of a thin epithelial film of blueberry fruit adhered to a graphite paste bed deposited onto a Pt electrode. Electrolyte, 2.5 mM $K_3Fe(CN)_6$ plus 2.5 mM $K_4Fe(CN)_6$ solution in air-saturated 0.10 M potassium phosphate buffer at pH 7.4. E_T = 0.30 V; a,c) E_S = 0.0 V; b,d) E_S = −1.0 V.

Scheme 1. Tentative scheme for the electrochemistry of delphinidin in the absence and in the presence of ROS. The grey area underlines the possible reaction scheme associated to the oxidation process A*.

Figure 1.

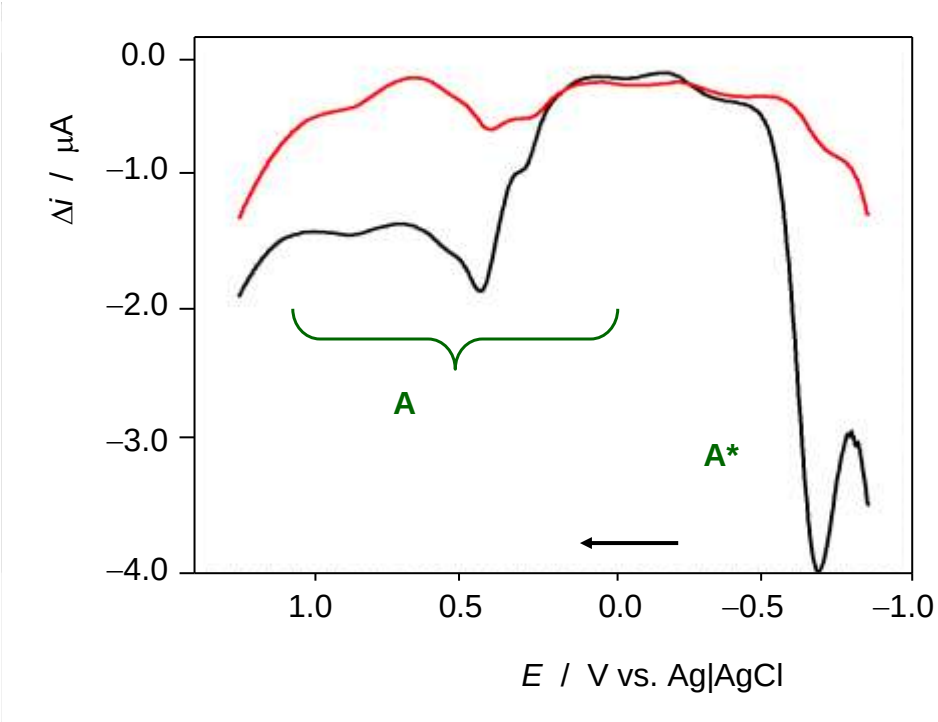

Figure 2.

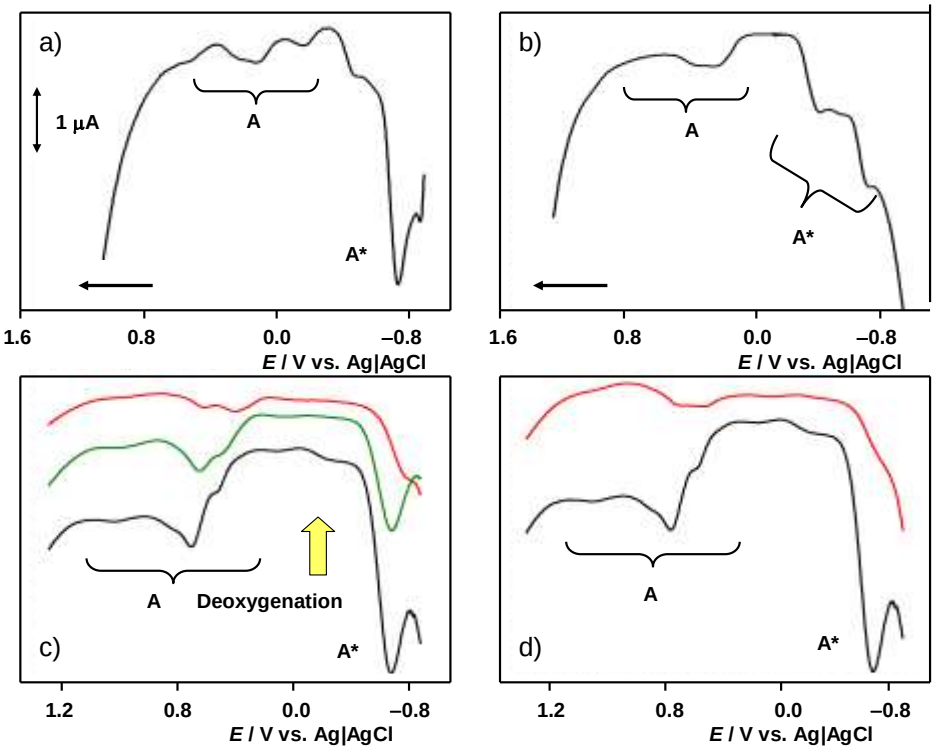
a)
1 µA
A
A*
1.6
0.8
0.0
–0.8
E / V vs. Ag|AgCl
b)
A
A*
1.6
0.8
0.0
–0.8
E / V vs. Ag|AgCl
A
Deoxygenation
c)
A*
1.2
0.8
0.0
–0.8
E / V vs. Ag|AgCl
A
d)
A*
1.2
0.8
0.0
–0.8
E / V vs. Ag|AgCl

Figure 3.

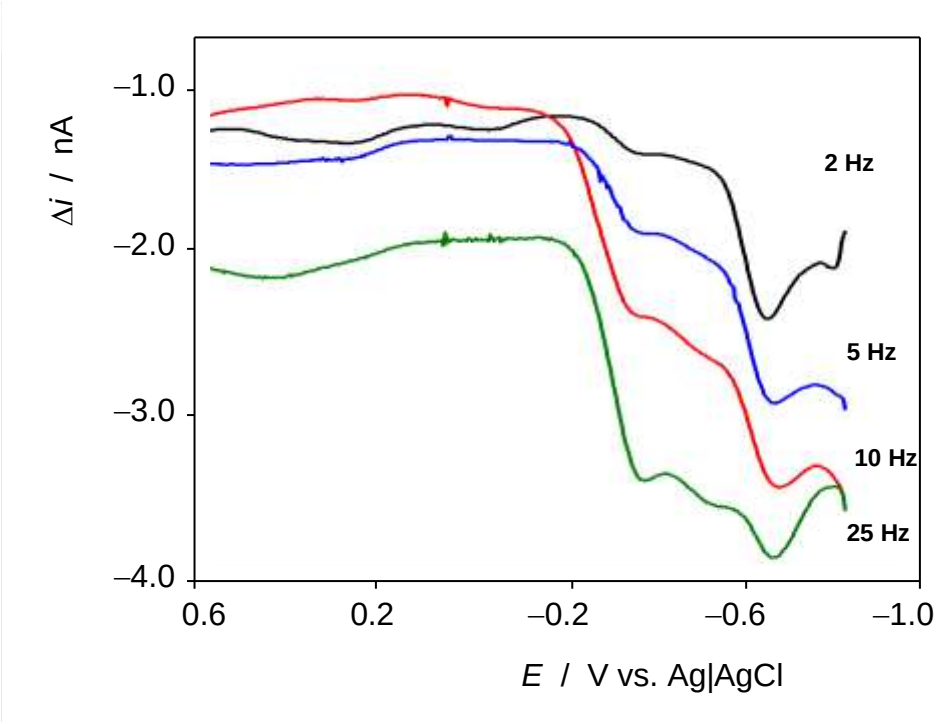

Figure 4.

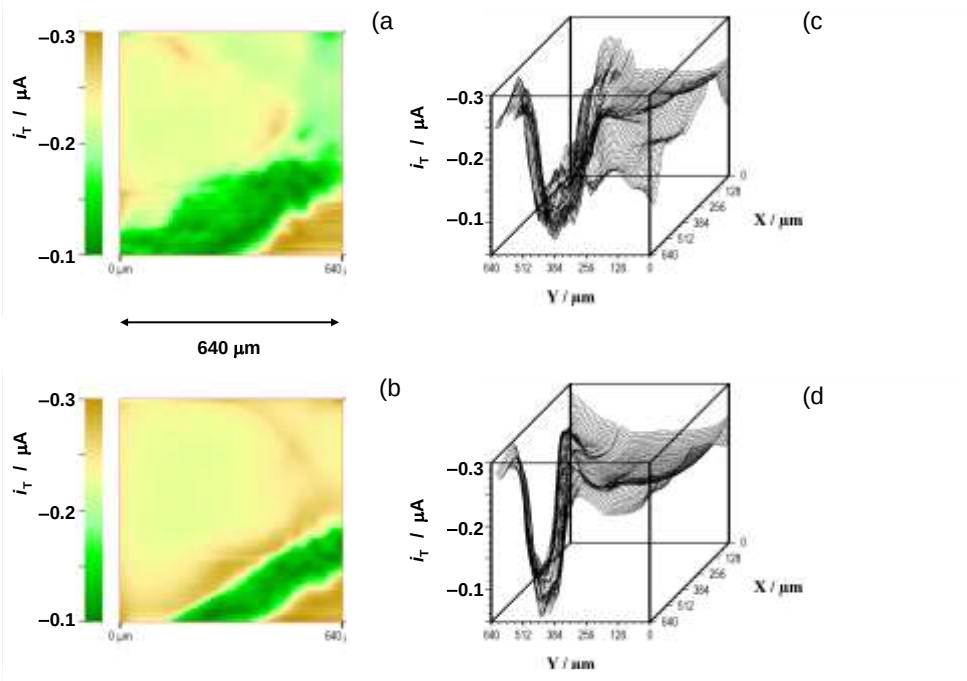

Scheme 1.